

Supplement materials:

The MS/MS fragmentation patterns of esculetin (Fig. S1A), rutin (Fig. S1B), daidzein (Fig. S1C), quercetin (Fig. S1D), apigenin (Fig. S1E), 16-hydroxyhexadecanoic acid (Fig. S1F), kaempferol-3-O-rutinoside (Fig. S1G), and kaempferol (Fig. S1H) were systematically analyzed using UPLC-Q-MS/MS. Esculetin displayed a characteristic protonated molecular ion $[M+H]^+$ at m/z 177.02, which underwent consecutive neutral losses of CO and OH to yield the predominant fragment ion at m/z 133.02 ($[M-H-CO-OH]^-$). Further fragmentation generated signature ions at m/z 105.03 ($C_7H_5O^+$) and 89.04 ($C_7H_5^+$), corresponding to sequential cleavages of the coumarin scaffold, while the base peak at m/z 77.04 ($C_6H_5^+$) confirmed the presence of a phenyl moiety. This coumarin derivative, ubiquitously distributed in medicinal plants including *Ceratostigma willmottianum*,¹ *Cortex Fraxini*,² has been extensively characterized as a multifunctional phytochemical. Recent studies confirm that esculetin exhibits dual antioxidant and anti-inflammatory effects through potent ROS scavenging activity and significant inhibition of key inflammatory enzymes.³ Particularly noteworthy is its nanomolar-range inhibitory activity against neurodegenerative targets, establishing esculetin as a promising neuroprotective agent with dual mechanisms targeting both amyloid genesis and cholinergic dysfunction.⁴ The peak at m/z 609.14 ($C_{27}H_{29}O_{16}^-$) corresponds to the protonated molecular ion of rutin, while the fragment ion at m/z 300.02 corresponds to the deprotonated quercetin formed after the loss of the glycosyl group.⁵ Daidzein fragmentation in negative mode produced: (a) precursor ion at m/z 253.05 ($[M-H]^-$, $C_{15}H_9O_4^-$); (b) m/z 224.04 ($[M-H-CO]^-$) through carbonyl loss; (c) m/z 196.04 ($[M-H-2CO]^-$); and (d) m/z 132.02 corresponding to the B-ring fragment $C_8H_4O^-$. Quercetin had a molecular ion peak $[M-H]^-$ of m/z 301.03 in the negative ion mode, and its stronger characteristic fragment ions at m/z 178.99, 151.00, and 107.01, consistent with previous reports.⁶ The protonated molecular ion peak of apigenin was located at m/z 271.03 and its characteristic fragment peaks at m/z 109.03.⁷

The MS/MS fragmentation patterns of luteolin (Fig. S2A), genistein (Fig. S2B), isorhamnetin (Fig. S2C), and cirsimaritin (Fig. S2D) were systematically analyzed using UPLC-Q-MS/MS. Luteolin demonstrated characteristic negative ion mode fragmentation: (a) molecular ion at m/z 285.04 ($[M-H]^-$, $C_{15}H_9O_6^-$); (b) m/z 217.05 via retro-Diels-Alder fragmentation; and (c) m/z 133.03 representing the dehydroxylated B-ring fragment.⁸ The signal response compound with protonation ion at m/z 269.04 yielding MS/MS ions at m/z 157.03, 135.04 and 107.01 was identified as Genistein,⁹ which belongs to one of the specific flavonoid components in BLDLF. Isorhamnetin exhibited a prominent molecular ion peak at m/z 315.05, along with a characteristic flavonoid fragment peak observed at m/z 151.00.¹⁰ Notably, the compound demonstrated a unique and intense signal at m/z 300.03, which represented a characteristic fragment resulting from the demethylation of the methoxy group ($-OCH_3$) on the B-ring. This distinctive mass spectral feature served as a reliable marker for differentiating isorhamnetin from other flavonoid compounds, such as quercetin. Cirsimaritin had a molecular ion peak at m/z 313.07 and a secondary characteristic ion peak at m/z 287.22.¹¹

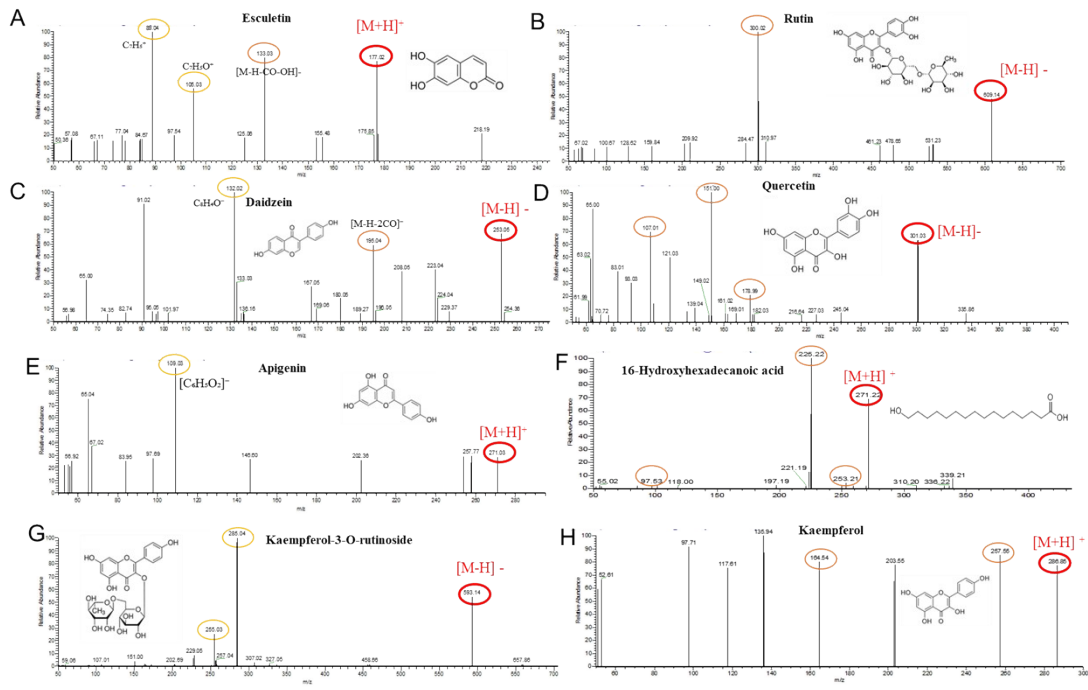


Fig. S1 The MS/MS fragmentation ions of compound Esculetin(A), rutin (B), daidzein (C), quercetin (D), apigenin (E), 16-hydroxyhexadecanoic acid (F), kaempferol-3-O-rutinoside (G), and kaempferol (H) by UPLC-Q-MS/MS

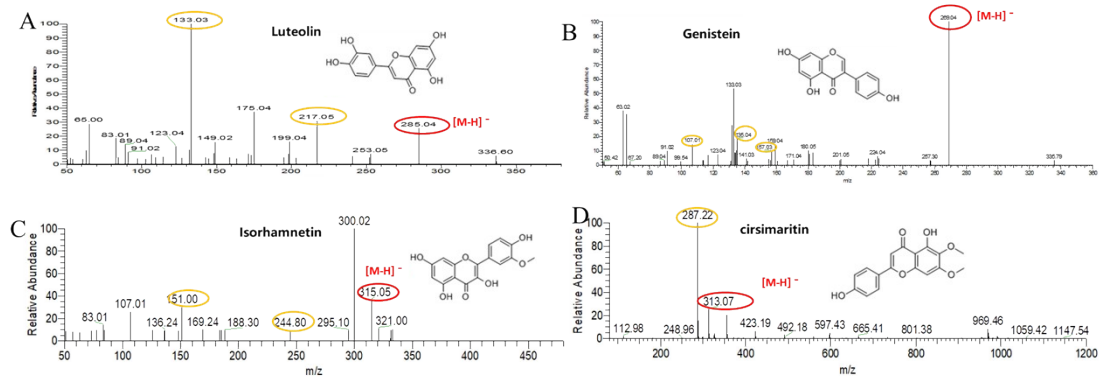


Fig. S2 The MS/MS fragmentation ions of compound luteolin (A), genistein (B), isorhamnetin (C), cirsimaritin (D) by UPLC-Q-MS/MS

After ethanol extraction, the surface of the DLF residue became rough and irregular, with many crevices and wrinkles appearing (Fig. S2B, supplementary material). This was because under the effect of ultrasound, the structure of plants was destroyed and the active components in plants were released.

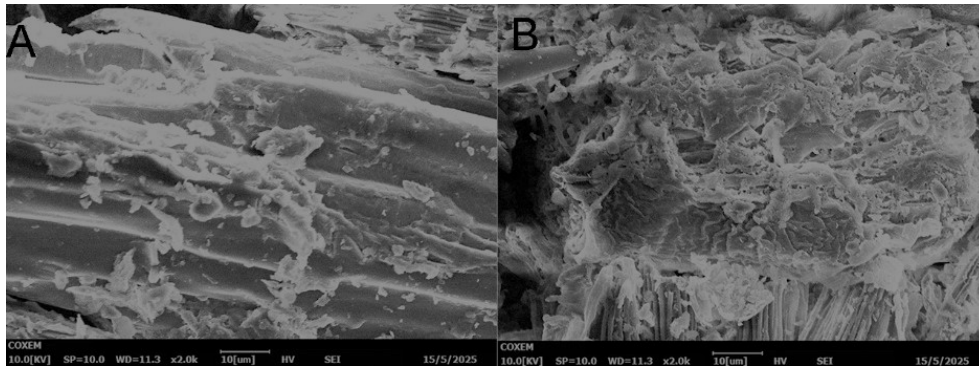


Fig. S3 Microscopic morphology comparison by SEM of the dried DLF (A), and the dried powder of DLF after extraction by 80% ethanol (B).

Reference:

1. Yue, J.-M.; Xu, J.; Zhao, Y.; Sun, H.-D.; Lin, Z.-W. Chemical Components from *Ceratostigma Willmottianum*. *J. Nat. Prod.* 1997, **60** (10), 1031–1033.
2. Wu, C.-R.; Huang, M.-Y.; Lin, Y.-T.; Ju, H.-Y.; Ching, H. Antioxidant Properties of Cortex *Fraxini* and Its Simple Coumarins. *Food Chem.* 2007, **104** (4), 1464–1471.
3. Zhang, Y.; An, Y.; He, X.; Zhang, D.; He, W. Esculetin Protects Human Corneal Epithelial Cells from Oxidative Stress through Nrf-2 Signaling Pathway. *Exp. Eye Res.* 2021, **202**, 108360.
4. Tahara, S.; Baba, N.; Matsuo, M.; Kaneko, T. Protective Effect of Epigallocatechin Gallate and Esculetin on Oxidative DNA Damage Induced by Psoralen plus Ultraviolet-a Therapy. *Biosci. Biotechnol., Biochem.* 2005, **69** (3), 620–622.
5. Coppin, J. P.; Xu, Y.; Chen, H.; Pan, M.-H.; Ho, C.-T.; Juliani, R.; Simon, J. E.; Wu, Q. Determination of Flavonoids by LC/MS and Anti-Inflammatory Activity in *Moringa Oleifera*. *J. Funct. Foods* 2013, **5** (4), 1892–1899.
6. Wang, W.; Liu, N.; Kang, Q.; Du, P.; Lan, Y.; Zhao, B.; Chen, Y.; Zhang, Q.; Li, H.; Zhang, Y.; Wu, Q. Simultaneous Determination by UPLC-MS/MS of Seven Bioactive Compounds in Rat Plasma after Oral Administration of Ginkgo Biloba Tablets: Application to a Pharmacokinetic Study. *J. Zhejiang Univ-sc. B* 2014, **15** (11), 929–939.
7. Seo, S.-W.; Choi, S. H.; Hong, J.-K.; Kim, K. M.; Kang, S. C.; Yoon, I.-S. Pharmacokinetics and Extensive Intestinal First-Pass Effects of Apigenin and Its Active Metabolite, Apigenin-7-O-Glucuronide, in Rats. *J. Pharm. Invest.* 2024, **54** (4), 467–481.
8. Mekky, R. H.; Abdel-Sattar, E.; Abdulla, M.-H.; Segura-Carretero, A.; Al-Khayal, K.; Eldehna, W. M.; Del Mar Contreras, M. Metabolic Profiling and Antioxidant Activity of Fenugreek Seeds Cultivars ‘Giza 2’ and ‘Giza 30’ Compared to Other Geographically-Related Seeds. *Food Chem.: X* 2024, **24**, 101819.
9. Yang, Z.; Zhu, W.; Gao, S.; Xu, H.; Wu, B.; Kulkarni, K.; Singh, R.; Tang, L.; Hu, M. Simultaneous Determination of Genistein and Its Four Phase II Metabolites in Blood by a Sensitive and Robust UPLC-MS/MS Method: Application to an Oral Bioavailability Study of Genistein in Mice. *J. Pharm. Biomed. Anal.* 2010, **53** (1), 81–89.
10. Wei, B.-B.; Chen, Z.-X.; Liu, M.-Y.; Wei, M.-J. Development of a UPLC-MS/MS Method for Simultaneous Determination of Six Flavonoids in Rat Plasma after Administration of *Maydis Stigma* Extract and Its Application to a Comparative Pharmacokinetic Study in Normal and

- Diabetic Rats. *Mol. : J. Synth. Chem. Nat. Prod. Chem.* 2017, **22** (8), 1267.
- (11) He, C.; Huang, W.; Xue, X.; Liang, Z.; Ye, H.; Li, K.; Yuan, X. UPLC-MS Fingerprints, Phytochemicals and Quality Evaluation of Flavonoids from *Abrus Precatorius* Leaves. *J. Food Compos. Anal.* 2022, **110**, 104585.